Astrocytic endfoot Ca^{2+} and BK channels determine both arteriolar dilation and constriction

Hélène Girouard[a,1], Adrian D. Bonev[a], Rachael M. Hannah[a], Andrea Meredith[b], Richard W. Aldrich[c,2], and Mark T. Nelson[a,2]

[a]Department of Pharmacology, University of Vermont, Burlington, VT 05405; [b]Department of Physiology, University of Maryland, Baltimore, MD 21201; and [c]Department of Neurobiology, University of Texas, Austin, TX 78712

Neuronal activity is thought to communicate to arterioles in the brain through astrocytic calcium (Ca^{2+}) signaling to cause local vasodilation. Paradoxically, this communication may cause vasoconstriction in some cases. Here, we show that, regardless of the mechanism by which astrocytic endfoot Ca^{2+} was elevated, modest increases in Ca^{2+} induced dilation, whereas larger increases switched dilation to constriction. Large-conductance, Ca^{2+}-sensitive potassium channels in astrocytic endfeet mediated a majority of the dilation and the entire vasoconstriction, implicating local extracellular K$^+$ as a vasoactive signal for both dilation and constriction. These results provide evidence for a unifying mechanism that explains the nature and apparent duality of the vascular response, showing that the degree and polarity of neurovascular coupling depends on astrocytic endfoot Ca^{2+} and perivascular K$^+$.

inwardly rectifying potassium channel | large-conductance calcium-sensitive potassium channel | neurovascular coupling

Functional hyperemia—a vasodilatory response to increased neuronal activity—ensures an adequate supply of nutrients and oxygen to active brain regions. Increased intracerebral blood flow in response to neuronal activity is a fundamental physiological process that is exploited diagnostically, forming the basis for techniques such as functional magnetic resonance imaging (fMRI), which uses both perfusion and blood-oxygenation level dependent (BOLD) contrast to map brain function.

Recent evidence indicates that neuronal activity is encoded in astrocytes in the form of dynamic intracellular calcium (Ca^{2+}) signals, which travel to astrocytic processes ("endfeet") encasing the arterioles in the brain. Astrocytic Ca^{2+} signaling has been implicated in the dilatory response of adjacent arterioles, which is in keeping with the functional linkage between neuronal activity and enhanced local blood flow (1–5). Paradoxically, however, astrocytic Ca^{2+} signals have also been linked to constriction (6, 7). The physiological significance of this response is not clear, but negative BOLD measurements may be indicative of vasoconstriction (8). The relationship between endfoot Ca^{2+} and vascular response is not known, and it is unclear whether or not changes in endfoot Ca^{2+} can account for the full spectrum of vascular responses to neuronal activity. Importantly, the mechanisms by which increases in astrocytic endfoot Ca^{2+} determine vascular response, dilation or constriction, remain unresolved.

Increases in astrocytic endfoot Ca^{2+} can potentially activate two major pathways: (*i*) cytoplasmic phospholipase A2 (PLA$_2$) and (*ii*) large-conductance, Ca^{2+}-sensitive potassium (BK) channels in the plasma membrane of astrocytic endfeet. Increased PLA$_2$ activity results in the production of arachidonic acid, which can be metabolized to vasoactive substances by a variety of enzymes within astrocytes (4, 5, 9); it has also been suggested that arachidonic acid diffuses to vascular smooth-muscle cells and is metabolized to 20-hydroxyeicosatetraenoic acid (HETE) (7), a vasoconstrictor that can inhibit smooth-muscle BK channels. Recent evidence indicates that activation of astrocytic BK channels by elevated endfoot Ca^{2+} leads to the release of potassium (K$^+$) into the perivascular space (1, 10), which acts through strong inward rectifier K$^+$ (K$_{ir}$) channels in the

sarcolemma of smooth-muscle cells to cause membrane hyperpolarization and induce vasodilation (1).

Results

Level of Astrocytic Endfoot Ca^{2+} Determines Dilation and Constriction in Brain Slices. We simultaneously measured astrocytic endfoot Ca^{2+} and diameters of adjacent arterioles in mouse cortical brain slices (Fig. 1*A* and Fig. S1). Arterioles were preconstricted (by 20–30%) with the thromboxane agonist, U46619 (125 nM), to induce physiological levels of arteriolar tone. Astrocytic Ca^{2+} was elevated by activating neurons with electrical field stimulation (EFS) or by uncaging Ca^{2+} in an astrocytic endfoot. In previous studies, only fractional changes in endfoot Ca^{2+} were measured (1–7). To circumvent this limitation, we bath-applied 20 mM Ca^{2+} and 10 μM ionomycin to determine the maximal fluorescence of Fluo-4, and then, we used this value to calculate intracellular Ca^{2+} concentration ([Ca^{2+}]$_i$) in the astrocytic endfoot (11). Under resting conditions, astrocytic endfoot [Ca^{2+}]$_i$ was 124 ± 6 nM (n = 43). Neuronal stimulation by low-voltage EFS elevated astrocytic endfoot [Ca^{2+}]$_i$ to 324 ± 16 nM and dilated adjacent arterioles by 21.3% ± 1.8% (n = 9) (Fig. 1*C*), which likely represents maximal dilation. EFS had no effect in the presence of the neuronal voltage-dependent sodium-channel blocker tetrodotoxin (TTX; 1 μM; n = 3), confirming neuronal dependence. Neuronal stimulation could also potentially affect vascular diameter through astrocytic pathways that do not involve Ca^{2+} or through direct effects mediated by interneurons (12). To bypass neurons and the astrocytic soma, we elevated astrocytic Ca^{2+} directly by uncaging Ca^{2+} in an individual endfoot. Under the photolysis conditions used, uncaging of a normal level of Ca^{2+} in a single endfoot elevated [Ca^{2+}]$_i$ to 350 ± 26 nM and increased arteriolar diameter by 22.0% ± 1.5% (n = 11) (Fig. 1 *A*–*C* and Movie S1).

The effects of higher levels of endfoot Ca^{2+} were explored by increasing neuronal stimulation, either by elevating EFS intensity or increasing the caged Ca^{2+} loading time. Higher-intensity EFS elevated astrocytic endfoot [Ca^{2+}]$_i$ to 732 ± 41 nM and switched dilation to a 29.9% ± 2.6% constriction (n = 8) (Fig. 1*C*). This effect was also blocked by TTX (1 μM; n = 3). Similarly, elevating Ca^{2+} by uncaging after a longer load period with caged Ca^{2+} increased astrocytic endfoot [Ca^{2+}]$_i$ to 832 ± 41 nM and caused constriction, decreasing arteriolar diameter by 28.6% ± 3.6% (n = 12) (Fig. 1 *A*–*C* and Movie S2). Collectively, these results indicate that the vascular response—arteriolar dilation or constriction—depends on the level of Ca^{2+} in the astrocytic endfoot (Fig. 1*C*).
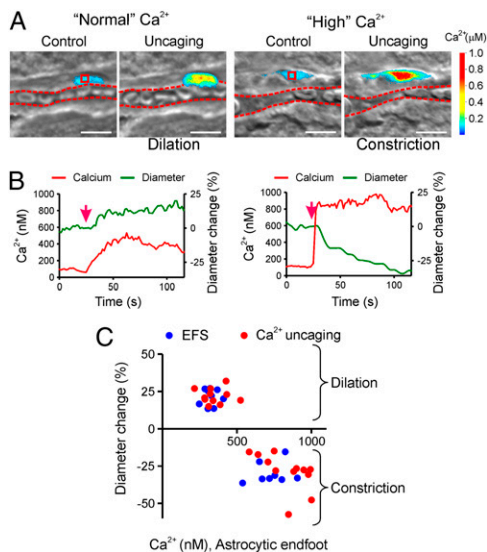
Fig. 1. Level of astrocytic endfoot Ca^{2+} determines arteriolar dilation and constriction. (*A*) An astrocytic endfoot on an arteriole in a brain slice loaded with the Ca^{2+} cage, DMNP-EDTA, before (Control) and after (Uncaging) two-photon Ca^{2+} uncaging in the region of interest (red squares). Shown are infrared differential interference contrast (IR-DIC) transmitted light images overlaid with pseudocolor-mapped $[Ca^{2+}]_i$ (based on Fluo-4 fluorescence). The slice shown on *Left* was loaded with DMNP-EDTA for 60 min, whereas the one shown on *Right* was loaded for 120 min. The vessel lumen is denoted by red dotted lines. (Scale bar: 10 μm.) (*B*) Traces showing the time course of changes in endfoot Ca^{2+} (red) and arteriole diameter (green) after Ca^{2+} uncaging. Normal Ca^{2+} increases led to dilation (*Left*), whereas high Ca^{2+} increases caused constriction (*Right*). Red arrows indicate the onset of Ca^{2+} uncaging. (*C*) Scatter plot illustrating the relationship between astrocytic endfoot $[Ca^{2+}]_i$ and the changes in the arteriole diameter after EFS (blue dots) and Ca^{2+} uncaging (red dots). Each dot represents an individual endfoot/arteriole (n = 40 arterioles in 35 brain slices from 22 animals).

Evoked Dilations and Constrictions Depend on BK Channels in Brain Slices. We have recently provided evidence that neuronal stimulation can cause vasodilation in rat brain slices through activation of BK channels in astrocytic endfeet and subsequent stimulation of K_{ir} channels in arteriolar smooth muscle (1). If endfoot Ca^{2+} acts through BK-channel stimulation, then inhibition of BK-channel function should reduce the vasodilatory response to elevated astrocytic endfoot $[Ca^{2+}]_i$. Consistent with this mechanism, the selective BK-channel blocker, paxilline (1 μM; *SI Methods*) (13), reduced vasodilations induced by low-intensity EFS stimulation by $75.5\% \pm 7.1\%$ ($n = 6$) and attenuated the dilatory response to endfoot Ca^{2+}, uncaging under low-load conditions by a similar $73.3\% \pm 12.4\%$ ($n = 5$) (Fig. 2 *A* and *C*). Paxilline did not affect EFS- or uncaging-induced elevations of astrocytic endfoot $[Ca^{2+}]_i$ ($n = 23$). These results support the idea that astrocytic endfoot Ca^{2+} activates BK channels to release K^+ onto arteriolar smooth muscle to cause vasodilation (Fig. S2).

To examine the hypothesis that the vasoconstriction caused by higher endfoot $[Ca^{2+}]_i$ is also mediated through activation of BK channels, we tested the effects of paxilline on vasoconstrictions induced by high-intensity EFS stimulation and high-load Ca^{2+} uncaging (Fig. S2). Paxilline blocked the entire constriction to EFS and uncaging and in each case, converted the response to a small dilation [$5.8\% \pm 3.8\%$ ($n = 5$) and $6.2\% \pm 4.1\%$ ($n = 7$) for EFS and uncaging, respectively] (Fig. 2 *B* and *C*). This small dilation was similar in magnitude to the residual dilation observed after inhibiting BK channels under conditions that induced vasodilation (Fig. 2C). In the absence of stimulation, paxilline nominally constricted ($5.3\% \pm 0.8\%$; $n = 4$) pre-constricted arterioles, likely reflecting inhibition of arteriolar

smooth-muscle BK channels, but had no significant effect on arterioles that were not preconstricted (Fig. 2D). The observation that BK-channel block inhibits Ca^{2+} uncaging-induced constriction but does not cause significant constriction by itself indicates that activation of astrocytic endfoot BK channels, rather than inhibition of smooth-muscle BK channels (7), is responsible for the observed vasoconstriction.

Raising External K^+ Causes Dilation and Constriction of Isolated Parenchymal Arterioles. Depending on its concentration, external K^+ ($[K^+]_o$) can rapidly dilate or constrict cerebral arteries through membrane-potential hyperpolarization and depolarization, respectively (1, 14, 15). The relationship between $[K^+]_o$ and diameter was determined in isolated mouse parenchymal arterioles (Fig. 3A). Elevating intravascular pressure to physiological levels (40 mmHg) induced myogenic tone, constricting parenchymal arterioles by $22.3\% \pm 1.9\%$ ($n = 8$). Raising $[K^+]_o$ from 3 mM to 8 mM caused a maximal dilation (Fig. 3A). The transition from dilation to constriction occurred at about 20 mM $[K^+]_o$ (Fig. 3A), which is the concentration at which the K^+ equilibrium potential (E_K) is similar to the smooth-muscle membrane potential (-45 mV) in physiological $[K^+]_o$ (3 mM) (1, 14, 15). The membrane-potential hyperpolarization induced by moderate elevations in $[K^+]_o$ is caused by activation of K_{ir} channels in the vascular smooth muscle (1, 14–16). We found that low concentrations (30 μM) of the K_{ir}-channel blocker, barium (Ba^{2+}; *SI Methods*), prevented the dilations caused by low K^+ but did not affect high K^+-induced constrictions (Fig. 3 *A* and *B*), which is similar to previous results from pial arteries (14, 15).

Raising External K^+ Switches Evoked Dilation to Constriction in Brain Slices. Our data indicate that there are potentially two polarity switches for converting dilation to constriction: (*i*) the level of astrocytic endfoot Ca^{2+}, and (*ii*) the perivascular level of K^+ (Fig. S2). We have previously shown that raising $[K^+]_o$ from normal levels (3 mM) to 8 mM hyperpolarizes arteriolar smooth muscle from approximately -44 mV to -80 mV and causes a very significant vasodilation (1) (Fig. 3A). To test the K^+-switch mechanism in the context of a brain slice, we measured responses to modest elevations of astrocytic $[Ca^{2+}]_i$ (300–400 nM) by uncaging endfoot Ca^{2+} in the presence of 3 mM and 8 mM $[K^+]_o$. Elevating $[K^+]_o$ to 8 mM converted endfoot Ca^{2+}-induced dilations to constrictions (Fig. 4), suggesting that 8 mM extracellular K^+ and BK channel-mediated K^+ efflux were additive, raising the local perivascular K^+ concentration above the dilation/constriction cross-over threshold. To prevent dilation to 8 mM K^+ (i.e., to maintain constant tone), we tested the effect of uncaging endfoot Ca^{2+} in the presence of the K_{ir}-channel blocker, Ba^{2+} (100 μM) (1, 15, 17). Elevating $[K^+]_o$ to 8 mM in the presence of Ba^{2+} also converted endfoot Ca^{2+}-induced dilation to constriction (Fig. 4), indicating that the level of tone did not affect the K^+-dependent polarity switch. The BK-channel inhibitor, paxilline (1 μM), completely blocked the constriction to low-level Ca^{2+} uncaging in 8 mM K^+/Ba^{2+} (Fig. 4). Neither the concentration of external K^+ (3 mM or 8 mM) nor the presence of Ba^{2+} and/or paxilline affected the level of uncaging-induced endfoot Ca^{2+} (Fig. 4C). These results are consistent with the concept that an elevation of astrocytic endfoot $[Ca^{2+}]_i$ activates BK channels, which release K^+ into the local perivascular space; this causes smooth-muscle hyperpolarization/dilation or depolarization/constriction, depending on the magnitude of K^+ release and ambient local $[K^+]_o$ (Fig. S2). The sensors of smooth-muscle membrane potential are sarcolemmal L-type voltage-dependent Ca^{2+} channels (VDCCs) (14, 18) (Fig. S2). The dihydropyridine VDCC antagonist, nitrendipine (5 μM), abrogated the vasoconstrictive effect of high-level endfoot Ca^{2+} uncaging ($n = 3$). Collectively, these results indicate that astrocytes regulate arteriolar tone through
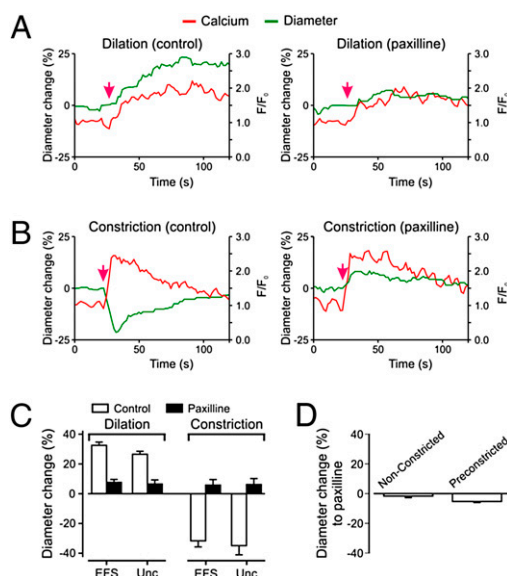
Fig. 2. BK channels are required for both vasodilations and constrictions induced by astrocytic endfoot Ca^{2+} increases. Time course of arteriolar diameter changes (green) to (A) normal and (B) high Ca^{2+} increases, measured as F/F_0 (red), after Ca^{2+} uncaging before and after BK-channel block with paxilline (1 μM). Red arrows indicate the onset of Ca^{2+} uncaging. (C) Summary of percentage diameter changes in response to astrocytic endfoot $[Ca^{2+}]_i$ increases before and after application of paxilline for 20 min. Both EFS and Ca^{2+} uncaging (DMNP-EDTA) were used to induce astrocytic $[Ca^{2+}]_i$ increases in brain slices. ($P < 0.01$ for all control versus paxilline groups; paired t test; $n = 5–7$ arterioles). (D) Paxilline alone caused a small constriction of arterioles preconstricted with 125 nM U46619 ($P < 0.05$; $n = 4$ arterioles) but did not affect the diameter of nonpreconstricted arterioles ($n = 5$).

modulation of smooth-muscle membrane potential with K_{ir}-mediated hyperpolarization inducing vasodilation by closing VDCCs and K^+-mediated depolarization activating smooth-muscle VDCC to induce vasoconstriction (Fig. S2).

Whisker Stimulation-Induced Increases in Cerebral-Blood Flow Depend on BK and K_{ir} Channels. To evaluate the implications of this neurovascular coupling mechanism in vivo, we used laser Doppler flowmetry (19–21) to measure cortical cerebral-blood flow (CBF) in mice in response to whisker stimulation or activation of astrocytes with the metabotropic glutamate receptor (mGluR) agonist, t-ACPD (50 μM). Whisker stimulation caused a 22.4% ± 0.3% increase in local CBF (Fig. 5 A and B). Application of the BK-channel blocker, paxilline (1 μM), or the K_{ir}-channel blocker, Ba^{2+} (100 μM), to the cranial window reduced whisker stimulation-induced increases in CBF by 50.7% ± 1.5% and 45.0% ± 1.5%, respectively (Fig. 5 A and B). The effects of paxilline on stimulation-induced CBF are similar to those previously reported for the

Fig. 3. Elevation of extracellular K^+ dilates and constricts isolated pressurized arterioles. Representative traces (A) and summary data (B) illustrating the relationship between $[K^+]_o$ and changes in diameter of isolated, pressurized (40 mmHg) parenchymal arterioles ($n = 8$). The K_{ir}-channel blocker, Ba^{2+} (30 μM), prevented dilations but not constrictions to $[K^+]_o$ ($n = 4$).

BK-channel blocker iberiotoxin (22). Consistent with the proposed BK-to-K_{ir} serial mechanism (Fig. S2), the combination of paxilline and Ba^{2+} was no more effective than either blocker alone (Fig. 5B). Paxilline, Ba^{2+}, and the combination did not have a significant effect on resting cortical CBF ($n = 5$), and previous reports have shown that BK-channel blockers have no effect on field potentials during whisker stimulation (22), ruling out an effect of paxilline on neurons.

To further examine the role of BK channels in neurovascular coupling, we tested the effects of paxilline and Ba^{2+} on whisker stimulation-induced increases in CBF in mice lacking the pore-forming α subunit of the BK channel ($Slo^{-/-}/Kcnma1^{-/-}$ mice) (23). Paxilline was without effect in the absence of BK channels, supporting the selectivity of paxilline (23) (Fig. 5C). Ba^{2+}, which substantially inhibited whisker stimulation-induced increases in CBF in wild-type mice, was ineffective in $Kcnma1^{-/-}$ mice (Fig. 5C), indicating that BK channels are required for K_{ir}-channel activation. Paxilline and Ba^{2+} did, however, reduce whisker stimulation-induced increases in CBF in mice lacking the smooth-muscle–specific β1 subunit of the BK channel (Fig. 5D), which is necessary for BK-channel functionality in vascular smooth muscle (24, 25). The fact that paxilline inhibited these responses in β1-KO animals, which have compromised smooth-muscle BK function, supports the idea that the inhibitory effect of paxilline is on astrocytic, and not smooth muscle, BK channels. Collectively, these in vivo results support the concept that endfoot BK and smooth-muscle K_{ir} channels act in series, forming a BK channel to K_{ir}-channel signaling module that has a significant role in neurovascular coupling (Fig. S2).

Raising External K^+ Switches an Astrocyte-Mediated Increase in CBF to a Decrease in CBF, Each of Which Requires Functional BK Channels. To test the possibility that an astrocyte-mediated hyperemic response could be converted to a decrease in cortical CBF similar to that observed in brain slices, we measured local CBF after stimulating astrocytes directly with the mGluR agonist, t-ACPD, in the presence of TTX (3 μM) to inhibit neuronal activity. As shown in Fig. 5 E and F, t-ACPD (50 μM) increased local CBF by 23.2% ± 1.9% ($n = 5$). When added alone, paxilline and Ba^{2+} reduced this increase in CBF by 59.3% ± 6.2% and 73.3% ± 3.8%, respectively (Fig. 5F). As was the case in brain slices, combined treatment with paxilline and Ba^{2+} was no more effective than either blocker alone (Fig. 5F). Elevating $[K^+]_o$ from 3 mM to 15 mM in the cranial-window superfusate increased CBF by 38.8% ± 2.2% ($n = 5$), an elevation that was blocked by Ba^{2+} (100 μM; $n = 5$). In the presence of Ba^{2+}, CBF was essentially unchanged by 15 mM $[K^+]_o$ (5.2% ± 1.7% increase; $n = 5$), similar to the effect of this combined treatment on arteriolar tone in brain slices. Elevating $[K^+]_o$ from 3 mM to 15 mM converted the t-ACPD–induced 23% increase in cortical CBF into a 22.6% ± 3.5% ($n = 5$) decrease (Fig. 5 E and F). Remarkably, in the presence of both elevated K^+ (15 mM) and Ba^{2+}, t-ACPD caused a dramatic decrease in local CBF to the point of ischemia (Fig. 4 E and F), suggesting that increases in astrocytic Ca^{2+} induced by t-ACPD translated into a significant release of K^+, which, with K_{ir} channels blocked, summed with bath K^+ to depolarize arteriolar smooth muscle and promote massive vasoconstriction. These t-ACPD–induced decreases in CBF (in 15 mM K^+) were completely blocked by paxilline in the presence or absence of Ba^{2+} (Fig. 5 E and F), consistent with the concept that functional BK channels are required for the decrease in local CBF caused by astrocyte activation.

Discussion

Emerging evidence increasingly points to a central role for astrocytic Ca^{2+} elevation in coupling neuronal activity to vasodilation in the brain (3, 5, 6, 26). However, the observation that, under some circumstances, an elevation in astrocytic Ca^{2+} can
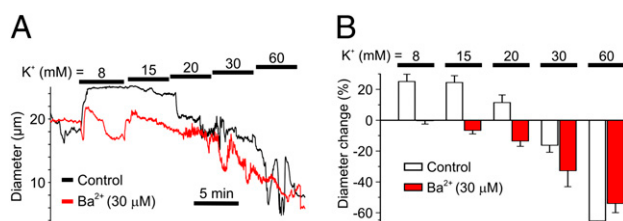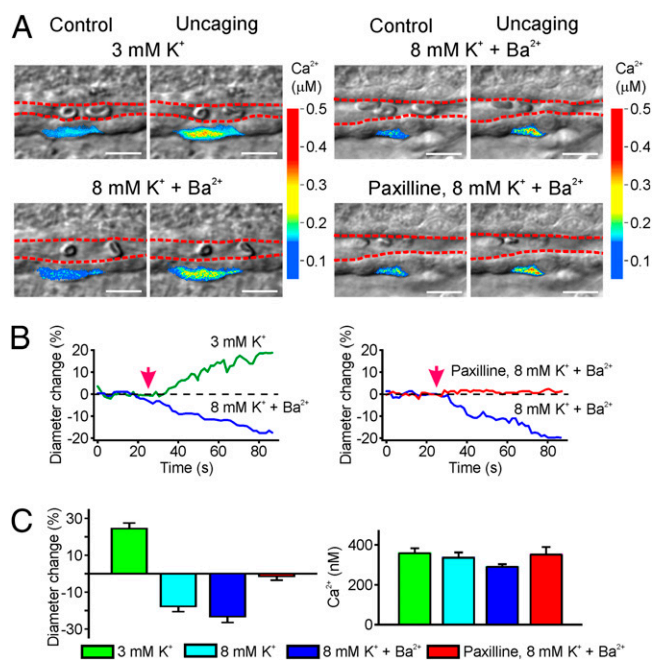
Fig. 4. Elevation of extracellular K^+ converts endfoot Ca^{2+}-induced dilations to constrictions. (*A* and *B*) Examples of simultaneous recording of changes in arteriolar diameter and $[Ca^{2+}]_i$ after Ca^{2+} uncaging in brain slices superfused with 3 mM or 8 mM K^+ showing the images (*A*) and time course of changes (*B*). Ba^{2+} (100 μM) was added to 8 mM K^+ aCSF to inhibit the vasodilation induced by elevated K^+. Elevation of $[K^+]_o$ from 3 mM to 8 mM converted endfoot Ca^{2+}-uncaging–induced dilation to constriction (*Left*) without affecting $[Ca^{2+}]_i$. Paxilline inhibited the endfoot Ca^{2+}-evoked constriction in 8 mM K^+ and Ba^{2+} (*Right*). Red arrows indicate the onset of Ca^{2+} uncaging. The lumen of an arteriole is denoted by the dotted red lines. (Scale bar: 10 μm.) (*C*) Summary of diameter (*Left*) and $[Ca^{2+}]_i$ (*Right*) changes in response to uncaging in brain slices perfused with aCSF containing 3 mM or 8 mM $[K^+]_o$ in the presence or absence of Ba^{2+} and paxilline ($n = 5$–10 arterioles). Paxilline inhibition of constriction was statistically significant ($P < 0.05$; $n = 5$). $[Ca^{2+}]_i$ after uncaging was not different for the four groups ($P < 0.05$). $[K^+]_o$ was elevated by increasing the KCl concentration at the expense of NaCl.

cause vasoconstriction (6, 7) poses a paradox. Our results effectively resolve this paradox, providing strong evidence that a single molecular mechanism is capable of causing both vasodilation and vasoconstriction. According to this unifying hypothesis, the vascular response depends on the level of astrocytic endfoot Ca^{2+}: moderate elevations in astrocytic $[Ca^{2+}]_i$ (300–400 nM) induce dilation of arterioles with tone and higher elevations (>700 nM) induce constriction (Fig. 1). The transition between evoked dilation and constriction occurs when the average endfoot $[Ca^{2+}]_i$ approximately doubles to 700–800 nM (Fig. 1*C*). This steep relationship could reflect the exquisitely high Ca^{2+} sensitivity of the astrocytic BK channel, which has been shown to exhibit a 16-fold increase in open probability with a doubling of $[Ca^{2+}]_i$ (27). BK-channel activation produces a concomitant increase in K^+ release from the astrocytic endfoot into the perivascular space, a restricted environment formed as a result of the envelopment of arterioles by astrocytic processes (Fig. S2) that encase >90% of the surface area of intracerebral arterioles (28). Because of this unique architectural feature, K^+ released by activated BK channels accumulates to produce local increases in K^+ that vary depending on the level of astrocytic BK-channel activity. On the arteriolar side, the smooth-muscle K_{ir} channel is activated by local extracellular K^+ in the 3–20 mM range, inducing very rapid membrane potential hyperpolarization and vasodilation. Interestingly, both elevation of external K^+ from 3 mM to 8 mM and calcium uncaging in the endfoot cause

essentially maximal dilation. This seems to reflect an off-on phenomenon attributable to the properties of the K_{ir} channel. Under resting conditions, the membrane potential (−45 mV) is very positive to the potassium-equilibrium potential (E_K; −102 mV), and K_{ir} channels are largely closed or off; activation of K_{ir} channels (e.g., by external K^+) leads to membrane hyperpolarization, which synergizes with K^+ to further activate K_{ir} channels (on), driving the membrane potential to new E_K and causing maximum dilation (1, 14, 15). At extracellular levels >20 mM, K^+ depolarizes smooth muscle, activating VDCCs and inducing vasoconstriction (14, 15). Presumably, the K^+ signal is terminated by active uptake of perivascular K^+ by Na/K ATPase and other Na^+-coupled K^+ transporters as well as by diffusion.

Importantly, the relationship between astrocytic $[Ca^{2+}]_i$ and vascular response is independent of the means by which Ca^{2+} is elevated: EFS and direct elevation of astrocytic endfoot $[Ca^{2+}]_i$ by uncaging Ca^{2+} both produced similar effects. The fact that elevating endfoot $[Ca^{2+}]_i$ by neuronal stimulation or Ca^{2+} uncaging evoked equivalent vascular responses indicates that other parallel, astrocyte/Ca^{2+}-independent processes need not be invoked to account for neurovascular coupling, and it argues that the effects of interneurons on vascular tone may be mediated through actions on astrocytic endfeet (3, 12).

Two candidate pathways have emerged as potential mediators of the Ca^{2+}-sensitive astrocytic endfoot mechanism that recent evidence suggests lies at the heart of the neurovascular coupling process: (*i*) Ca^{2+} activation of PLA_2 with the release of vasodilatory prostaglandin compounds (e.g., PGE_2) (2, 4, 5, 9, 28), and (*ii*) Ca^{2+} activation of endfoot BK channels, leading to the release of K^+ into the perivascular space (1, 3). The concentration-dependent ability of extracellular K^+ ions to very rapidly induce both vasodilation and vasoconstriction, described above, has led us to focus on this latter mechanism, which exhibits all of the features necessary for rapid, effective neurovascular coupling. However, our results clearly indicate that this is not the only mechanism at work. Depending on the experimental approach used, ~30% (brain slices) to 50% (CBF in vivo) of the vasodilatory response to elevated astrocytic endfoot $[Ca^{2+}]_i$ was insensitive to inhibitors of BK and K_{ir} channels. This paxilline/Ba^{2+}-resistant component of vasodilation is sensitive to COX inhibition with 10 μM indomethacin (1), consistent with the studies of others (4, 5, 28). In brain slices, this residual dilation was comparable in magnitude with the dilation observed after blocking BK channels under stimulus conditions that induced vasoconstriction, suggesting that both experimental paradigms revealed a common BK-channel–independent vasodilatory mechanism (Fig. S2). As suggested by these findings, PLA_2 and BK channel mechanisms are not mutually exclusive. They may, in fact, intersect, because products of arachidonic acid [e.g., 20-HETE, epoxyeicosatetraenoic acids (EETs), PGE_2] could directly or indirectly modulate BK channels, including those in astrocytes, or indirectly modulate the smooth-muscle response to the incoming K^+ signal by altering smooth-muscle membrane potential and smooth-muscle Ca^{2+} and/or tone (9, 29–31).

Strikingly, the CBF response to whisker stimulation in *Kcnma1*$^{−/−}$ mice was comparable with that in wild-type mice. This suggests that a non-BK/K_{ir}-channel pathway, presumably a PLA_2-dependent mechanism, has compensated for the loss of the BK channel during development, showing a remarkable plasticity of the neurovascular coupling process. Interestingly, whisker stimulation-induced increases in CBF also remain intact after disruption of the $PLA_2\alpha$ gene (32). Although this result may indicate that the $PLA_2\alpha$ isoform is not involved in neurovascular coupling, as the authors suggest, it may be further evidence for developmental plasticity of neurovascular coupling mechanisms.

Although there is an emerging consensus view of the role of astrocytes and the centrality of Ca^{2+}-dependent mechanisms in neurovascular coupling, there are divergent observations that
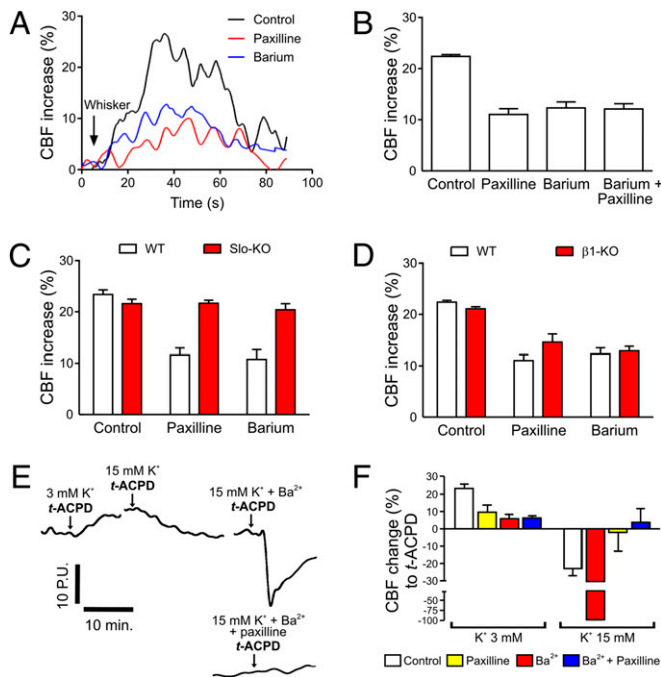
Fig. 5. Regulation of CBF responses to whisker stimulation and astrocyte activation by BK channels, Kir channels, and $[K^+]_o$. (*A*) Local administration of the BK-channel blocker, paxilline (1 μM), or K_{ir}-channel blocker, Ba^{2+} (100 μM), significantly reduced cortical CBF response to whisker stimulation and astrocyte activation (50 μM t-ACPD) in wild-type mice (*A*, *B*, and *F*) and in mice lacking the β1 subunit of the BK channel (*P* < 0.05; one-way ANOVA; *n* = 5–6 mice/group) (*D*). It did not significantly reduce cortical CBF response in mice lacking the α subunit of the BK channel (*n* = 4–5 mice/group). (*C*) In all cases, the effects of paxilline and barium on CBF were not statistically different from paxilline or barium alone. Panel *A* shows representative traces of the effects of BK- and K_{ir}-channel blockers on the whisker stimulation-induced increase in CBF. Paxilline or Ba^{2+} was superfused over the cranial window for 20 min before and after whisker stimulation. (*E*) Representative traces show the effects of 3 mM and 15 mM KCl on the CBF responses to astrocyte stimulation with t-ACPD in the presence or absence of Ba^{2+} and paxilline; TTX (3 μM) was included to block potential neuronal effects. (*F*) Summary data of t-ACPD–induced changes in CBF in the presence of 3 mM and 15 mM $[K^+]_o$, illustrating the ability of $[K^+]_o$ to convert hyperemic responses to decreases in CBF, which are also blocked by paxilline (*P* < 0.05; *n* = 5 mice/group).

likely reflect differences in experimental preparations and methodologies. Important in this context is the degree of vascular tone, which can affect the response to incoming astrocytic signals (29). In vessels that are not preconstricted, elevation of astrocytic $[Ca^{2+}]_i$ has been shown to induce constriction in brain slices from mouse and postnatal rats (7), but dilation is observed in preconstricted vessels. The nature of the vessel also determines the degree of response; whereas preconstricted arterioles exhibit rapid and robust dilations ex vivo and in vivo (1, 4–6), venules exhibit very small and sluggish changes (33, 34). This is not surprising, because although cerebral venules are decorated with occasional pericytes, they have little or no smooth muscle (33). Oxygen tension has also recently been reported to influence vascular responses, affecting the polarity of the vessel response to elevated astrocytic $[Ca^{2+}]_i$ (2). In this latter study, brain slices were superfused with artificial cerebrospinal fluid (aCSF) that initially contained 95% oxygen; reducing pO_2 to 20% shifted vessel constriction to dilation. In this case, the vessels were not preconstricted, and the responses were small (<10% constriction) and occurred slowly (over minutes). More typically, arterioles superfused with aCSF initially equilibrated in 95% oxygen dilate rapidly after elevation of astrocytic $[Ca^{2+}]_i$ (1, 3, 4, 6, 28). In any case, preconstricted arterioles exposed to constant pO_2 in slices

or in the retina are capable of dilating or constricting to an elevation of astrocytic $[Ca^{2+}]_i$ (6, 7). As shown here, the nature of this response—dilation or constriction—depends on the level of endfoot Ca^{2+}, which was not determined in these previous studies. It is also important to recognize that the pO_2 in the slice is not the same as that in the superfusate. Passage of superfusate through tubing and exposure to air reduces the actual level of oxygen in aCSF on the slice to considerably below 95% (to ~35% in our studies) (29).

One implication of our study is that BK-channel–mediated K^+ release and external levels of K^+ sum to determine the vascular outcome. As predicted, we found that modestly elevating $[K^+]_o$ under stimulus conditions that normally caused dilation in brain slices or increased CBF in vivo converted dilations to constrictions and increases in CBF to decreases in CBF. Thus, depending on the ambient level of bulk external K^+, stimuli that dramatically elevate endfoot $[Ca^{2+}]_i$ may convert vasodilation to vasoconstriction. This situation might develop under pathological conditions that result in elevated extracellular K^+, such as spreading depression, hypoxia/ischemia, trauma, hypoglycemia, and hyperammonemia (35–37). It has recently been reported that astrocytic Ca^{2+} signaling is elevated in an Alzheimer's disease model (38), suggesting the possibility of compromised functional hyperemia through conversion of local dilatory responses to vasoconstriction. Thus, our results serve as a possible mechanistic framework for understanding how K^+ dysregulation or astrocyte Ca^{2+} dysfunction contribute to neuropathologies.

Methods

Animal Procedures and Brain Slice Preparation. After euthanizing with an overdose of isoflurane, 2–3-month-old male C57BL6 mice were decapitated, and brains were rapidly removed and placed into 4 °C aCSF containing 125 mM NaCl, 3 mM KCl, 26 mM NaHCO₃, 1.25 mM NaH₂PO₄, 2 mM CaCl₂, 1 mM MgCl₂, 4 mM glucose, and 400 μM L-ascorbic acid (added to reduce cell swelling associated with oxidative stress). The pH of this solution, equilibrated with 95% O₂/5% CO₂, was 7.4. The brain was cut into 160-μm thick coronal slices using a vibratome (VT1000S; Leica). Slices were stored in aCSF at room temperature (20–22 °C) before loading dye or caged Ca²⁺ (1, 3, 26). All animal procedures were approved by the University of Vermont Office of Animal Care Management and are in accordance with the National Institutes of Health *Guide for the Care and Use of Laboratory Animals*.

Imaging of Ca²⁺ and Arteriolar Diameter. Arterioles in layers 2–5 of the cortex showed to arise from cortical-surface pial arteries were selected for experimentation. In brain-slice preparations, arterioles are readily identifiable by their wall thickness (~5 μm; i.e., the thickness of a single smooth-muscle cell layer), sinuous morphology, presence of a continuous smooth-muscle layer oriented perpendicular to endothelial cells, and presence of spontaneous oscillations (1, 3, 39) (Fig. S1). These properties clearly distinguish arterioles from venules, which do not have smooth muscle, are more uniformly tube-shaped, and are decorated by longitudinally oriented pericytes (Fig. S1). Arteriolar internal (luminal) diameter was determined from the distance between at least three paired points across the arteriole directly adjacent to an identified endfoot. Baseline diameter was obtained from 15 images immediately preceding stimulation. In each experiment, the number of arterioles studied corresponds to the number of slices used.

Cortical slices were loaded with the nonratiometric Ca²⁺ indicator, Fluo-4-acetoxymethyl (AM) (10 μM; Invitrogen), and 2.5 μg/mL pluronic acid in aCSF for 60 min at 29 °C. In some experiments, slices were coloaded with the caged Ca²⁺ compound, 1-[4,5-dimethoxy-2-nitrophenyl]-EDTA-AM (DMNP-EDTA-AM, 10 μM; Interchim), for 60–120 min using the same loading conditions and keeping Fluo-4 loading time at 60 min. Under these conditions, AM dyes primarily load astrocytes. After the incubation period, slices were washed and placed in aCSF until used.

At the time of the experiment, a slice was transferred to a perfusion chamber and continuously perfused with 35 °C aCSF containing the thromboxane A2 receptor agonist, 9,11-dideoxy-11α,9α-epoxymethanoprostaglandin F2α (U46619; 125 nM), to maintain vascular tone throughout the course of the experiment. This maneuver mimics the partially constricted state (20–30%) of the arteriole in vivo and allows both vasodilation and vasoconstriction to be measured (26, 40). aCSF oxygen levels after passing through the tubing into the slice chamber were reduced from 95% to ~35%, which was measured with an OM-4 oxygen

meter and electrode. Arteriolar diameter/morphology and intracellular Ca^{2+} were determined simultaneously. Ca^{2+} was imaged using a two-photon laser-scanning microscope (BioRad Radiance 2100 MP) directly coupled to a Coherent Chameleon Ti:sapphire laser (140-fs pulses, 1.5 W) and an Olympus BX51WI upright microscope equipped with a 20× water-dipping objective (Olympus XLUMPlan FI; 0.95 N.A.). Arteriolar diameter/morphology was measured using a transmitted light detector and infrared differential inter-ference contrast (IR-DIC) microscopy. Imaging protocols and acquisition were controlled using BioRad LaserSharp 2000 software. Fluo-4 was excited at 820 nm, and fluorescence emission was collected using a 575/150-nm bandpass filter. For experiments using caged Ca^{2+}, the laser was set at 730 nm, which allows for simultaneous excitation of Fluo-4 (41) and photolysis of the Ca^{2+} cage, DMNP-EDTA (42). Arterioles located ~50 μm (range = 20–80 μm) below

the cut surface of the brain slice with preconstricted external diameters in the 15–20-μm range were used for experiments.

For detailed experimental information regarding Ca^{2+} uncaging and neuronal stimulation in brain slices, endfoot Ca^{2+} quantification, diameter measurements of isolated pressurized parenchymal arterioles, in vivo experiment, reagents, and statistical analysis, please refer to *SI Methods*.

1. Filosa JA, et al. (2006) Local potassium signaling couples neuronal activity to vasodilation in the brain. *Nat Neurosci* 9:1397–1403.
2. Gordon GR, Choi HB, Rungta RL, Ellis-Davies GC, MacVicar BA (2008) Brain metabolism dictates the polarity of astrocyte control over arterioles. *Nature* 456:745–749.
3. Straub SV, Bonev AD, Wilkerson MK, Nelson MT (2006) Dynamic inositol trisphosphate-mediated calcium signals within astrocytic endfeet underlie vasodilation of cerebral arterioles. *J Gen Physiol* 128:659–669.
4. Takano T, et al. (2006) Astrocyte-mediated control of cerebral blood flow. *Nat Neurosci* 9:260–267.
5. Zonta M, et al. (2003) Neuron-to-astrocyte signaling is central to the dynamic control of brain microcirculation. *Nat Neurosci* 6:43–50.
6. Metea MR, Newman EA (2006) Glial cells dilate and constrict blood vessels: A mechanism of neurovascular coupling. *J Neurosci* 26:2862–2870.
7. Mulligan SJ, MacVicar BA (2004) Calcium transients in astrocyte endfeet cause cerebrovascular constrictions. *Nature* 431:195–199.
8. Devor A, et al. (2007) Suppressed neuronal activity and concurrent arteriolar vasoconstriction may explain negative blood oxygenation level-dependent signal. *J Neurosci* 27:4452–4459.
9. Koehler RC, Roman RJ, Harder DR (2009) Astrocytes and the regulation of cerebral blood flow. *Trends Neurosci* 32:160–169.
10. Price DL, Ludwig JW, Mi H, Schwarz TL, Ellisman MH (2002) Distribution of rSlo Ca2+-activated K+ channels in rat astrocyte perivascular endfeet. *Brain Res* 956:183–193.
11. Maravall M, Mainen ZF, Sabatini BL, Svoboda K (2000) Estimating intracellular calcium concentrations and buffering without wavelength ratioing. *Biophys J* 78:2655–2667.
12. Hamel E (2006) Perivascular nerves and the regulation of cerebrovascular tone. *J Appl Physiol* 100:1059–1064.
13. Imlach WL, et al. (2008) The molecular mechanism of "ryegrass staggers," a neurological disorder of K+ channels. *J Pharmacol Exp Ther* 327:657–664.
14. Knot HJ, Nelson MT (1998) Regulation of arterial diameter and wall [Ca2+] in cerebral arteries of rat by membrane potential and intravascular pressure. *J Physiol* 508:199–209.
15. Knot HJ, Zimmermann PA, Nelson MT (1996) Extracellular K(+)-induced hyperpolarizations and dilatations of rat coronary and cerebral arteries involve inward rectifier K(+) channels. *J Physiol* 492:419–430.
16. Zaritsky JJ, Eckman DM, Wellman GC, Nelson MT, Schwarz TL (2000) Targeted disruption of Kir2.1 and Kir2.2 genes reveals the essential role of the inwardly rectifying K(+) current in K(+)-mediated vasodilation. *Circ Res* 87:160–166.
17. Quayle JM, McCarron JG, Brayden JE, Nelson MT (1993) Inward rectifier K+ currents in smooth muscle cells from rat resistance-sized cerebral arteries. *Am J Physiol* 265:C1363–C1370.
18. Rubart M, Patlak JB, Nelson MT (1996) Ca2+ currents in cerebral artery smooth muscle cells of rat at physiological Ca2+ concentrations. *J Gen Physiol* 107:459–472.
19. Lindauer U, Villringer A, Dirnagl U (1993) Characterization of CBF response to somatosensory stimulation: Model and influence of anesthetics. *Am J Physiol* 264:H1223–H1228.
20. Girouard H, Park L, Anrather J, Zhou P, Iadecola C (2007) Cerebrovascular nitrosative stress mediates neurovascular and endothelial dysfunction induced by angiotensin II. *Arterioscler Thromb Vasc Biol* 27:303–309.
21. Girouard H, Meredith A, Aldrich R, Nelson M (2008) Roles of BK and Kir channels in the coupling of neural activity to vasodilation in the somatosensory cortex in vivo. *FASEB J* 22:lb634.

22. Gerrits RJ, Stein EA, Greene AS (2002) Ca(2+)-activated potassium (K(Ca)) channel inhibition decreases neuronal activity-blood flow coupling. *Brain Res* 948:108–116.
23. Meredith AL, Thorneloe KS, Werner ME, Nelson MT, Aldrich RW (2004) Overactive bladder and incontinence in the absence of the BK large conductance Ca2+-activated K+ channel. *J Biol Chem* 279:36746–36752.
24. Plüger S, et al. (2000) Mice with disrupted BK channel beta1 subunit gene feature abnormal Ca(2+) spark/STOC coupling and elevated blood pressure. *Circ Res* 87:E53–E60.
25. Brenner R, et al. (2000) Vasoregulation by the beta1 subunit of the calcium-activated potassium channel. *Nature* 407:870–876.
26. Filosa JA, Bonev AD, Nelson MT (2004) Calcium dynamics in cortical astrocytes and arterioles during neurovascular coupling. *Circ Res* 95:e73–e81.
27. Horrigan FT, Aldrich RW (2002) Coupling between voltage sensor activation, Ca2+ binding and channel opening in large conductance (BK) potassium channels. *J Gen Physiol* 120:267–305.
28. Iadecola C, Nedergaard M (2007) Glial regulation of the cerebral microvasculature. *Nat Neurosci* 10:1369–1376.
29. Blanco VM, Stern JE, Filosa JA (2008) Tone-dependent vascular responses to astrocyte-derived signals. *Am J Physiol Heart Circ Physiol* 294:H2855–H2863.
30. Harder DR, et al. (1994) Formation and action of a P-450 4A metabolite of arachidonic acid in cat cerebral microvessels. *Am J Physiol* 266:H2098–H2107.
31. Zou AP, et al. (1996) Stereospecific effects of epoxyeicosatrienoic acids on renal vascular tone and K(+)-channel activity. *Am J Physiol* 270:F822–F832.
32. Kitaura H, et al. (2007) Roles of nitric oxide as a vasodilator in neurovascular coupling of mouse somatosensory cortex. *Neurosci Res* 59:160–171.
33. Edvinsson L, Högestätt ED, Uddman R, Auer LM (1983) Cerebral veins: Fluorescence histochemistry, electron microscopy, and in vitro reactivity. *J Cereb Blood Flow Metab* 3:226–230.
34. Lee SP, Duong TQ, Yang G, Iadecola C, Kim SG (2001) Relative changes of cerebral arterial and venous blood volumes during increased cerebral blood flow: Implications for BOLD fMRI. *Magn Reson Med* 45:791–800.
35. Hansen AJ (1985) Effect of anoxia on ion distribution in the brain. *Physiol Rev* 65:101–148.
36. Leis JA, Bekar LK, Walz W (2005) Potassium homeostasis in the ischemic brain. *Glia* 50:407–416.
37. Sugimoto H, Koehler RC, Wilson DA, Brusilow SW, Traystman RJ (1997) Methionine sulfoximine, a glutamine synthetase inhibitor, attenuates increased extracellular potassium activity during acute hyperammonemia. *J Cereb Blood Flow Metab* 17:44–49.
38. Kuchibhotla KV, Lattarulo CR, Hyman BT, Bacskai BJ (2009) Synchronous hyperactivity and intercellular calcium waves in astrocytes in Alzheimer mice. *Science* 323:1211–1215.
39. Mayhew JE, et al. (1996) Cerebral vasomotion: A 0.1-Hz oscillation in reflected light imaging of neural activity. *Neuroimage* 4:183–193.
40. Brown LA, Key BJ, Lovick TA (2002) Inhibition of vasomotion in hippocampal cerebral arterioles during increases in neuronal activity. *Auton Neurosci* 95:137–140.
41. Xu C, Zipfel W, Shear JB, Williams RM, Webb WW (1996) Multiphoton fluorescence excitation: New spectral windows for biological nonlinear microscopy. *Proc Natl Acad Sci USA* 93:10763–10768.
42. Brown EB, Shear JB, Adams SR, Tsien RY, Webb WW (1999) Photolysis of caged calcium in femtoliter volumes using two-photon excitation. *Biophys J* 76:489–499.